An Integrated Approach to the Biological Reactor–Sedimentation Tank System

Serena Conserva [1], Fabio Tatti [1], Vincenzo Torretta [2] , Navarro Ferronato [2,* and Paolo Viotti [1]

[1] Department of Civil, Building and Environmental Engineering (DICEA), Sapienza University of Rome, Via Eudossiana 18, 00184 Rome, Italy; serena.conserva@uniroma1.it (S.C.); fabio.tatti@uniroma1.it (F.T.); paolo.viotti@uniroma1.it (P.V.)

[2] Department of Theoretical and Applied Sciences (DISTA), University of Insubria, Varese, Via G.B. Vico 46, 21100 Varese, Italy; vincenzo.torretta@uninsubria.it

* Correspondence: nferronato@uninsubria.it

check for updates

Abstract: Secondary clarifiers are demanded to separate solids created in activated sludge biological processes to achieve both a clarified effluent and to manage the biological processes itself. Indeed, the biological process may influence the sludge characteristics, and conversely, the settling efficiency of the sedimentation basin plays an important role on the biological process in the activated sludge system. The proposed model represents a tool for better addressing the design and management of activated sludge system in wastewater treatment plants. The aim is to develop a numerical model which takes into account both the conditions in the biological reactor and the sludge characteristics coupled to the hydrodynamic behavior of a clarifier tank. The obtained results show that the different conditions in the reactor exert a great influence on the sedimentation efficiency.

Keywords: activate sludge; numerical model; secondary clarifier; treatment efficiency

1. Introduction

Sedimentation basins are used in wastewater treatment plants to separate suspended solids from water. Secondary clarifiers are used to remove settleable solids created in biological processes such as the activate sludge process being an active part of the process itself. Settling basins are mainly designed using simple rules based on detention time, overflow rate, and solid loadings, which ensure that flow velocities in the basins are sufficiently low to allow solid particles to settle and to be removed, and yet sufficiently high so that the basin volumes are not excessively large.

Compliance with the effluent requirements depends greatly on the efficiency of the secondary clarifiers. The tank performance is strongly influenced by hydrodynamic processes together with physical effects, such as density-driven flow, gravity sedimentation, flocculation, and thickening.

Development and application of numerical models to calculate the velocity pattern in sedimentation tanks assumes a remarkable importance because it is proven that the actual characteristics of flow differ strongly from the supposed uniform distribution, and they have a relevant influence on the settling efficiency.

Since the 1970s, simulations of the flow field in rectangular sedimentation tanks have been carried out [1–6]. Research activities have been focused on the behavior of sedimentation and flotation of activated sludge in turbulent flows, mainly with numerical models able to simulate detailed geometries and boundary conditions, on the structure of inlet and removal process. The numerical models relative to sedimentation tanks operating in conditions of uniform density can be distinguished mainly for the adopted model of turbulence; for the choice of the boundary conditions; for the discretization method;

and for the procedure used in the numerical resolution. The precursor in flow fields modeling in primary sedimentation tanks was the author of [2]. In his work, the turbulent viscosity was calculated on the base of the Prandtl's theory on the mixing length. In 1981, the author of [7] proposed a model for primary sedimentation distinguishing the velocity field from the concentration one and introduced the hypothesis that the two fields can be solved separately (not coupling hypothesis). They adopted a finite elements technique to determine the flow and calculated the eddy diffusivity coefficient (v_t) through the turbulent kinetic energy "k" and its viscous dissipation "ε" (k-ε model proposed by [8]). The k-ε model is the most used turbulent model due to its robustness and reasonable accuracy for the prediction of turbulent flow in secondary sedimentation tanks [9–17].

In 1983, the authors of [18] developed a numerical model for rectangular sedimentation tanks, determining the velocity field and the suspended solids distribution. The authors used the hypothesis that the flow is a bi-phase turbulent flow. In primary sedimentation basins, where the inlet concentration is low, the simulation of liquid phase can be considered separately from the solid one, assuming that the particle presence does not influence the mechanisms of fluid flow, with the exception of turbulent mixing. Although the flow is generally three-dimensional, the bi-dimensional representation in the forecast of the velocity distribution was thought adapted, also for the computational difficulty of the 3D representation.

Several authors considered models in which the influence of densiometric forces of mass on the hydrodynamic field is neglected and the equations of the motion are solved independently from the transport one [5,9,19–21].

A mathematical model to predict, by direct computation, the behavior of the bottom current and surface return flow and simultaneously determine their distributional effects on the sedimentation process was proposed by [22].

Many studies were carried out to investigate the role of the reaction baffle position on the performance of the sedimentation unit [13,23–26]. In particular, the author of [23] proposed a numerical model for estimating the velocity field and suspended solids distribution in a secondary circular clarifier with density differences. The model predicted an important phenomenon known as the density waterfall that occurs for large radius baffles. A comparison of the solid's concentration distribution for a tank with a small skirt radius shows that this one reduces the density waterfall effect and significantly improves the clarifier performances.

Other authors assumed that particles settle as in a monodisperse suspension, with a velocity dependent on the concentration even in zones where the sludge is diluted [23,27–29], simulated a tertiary sedimentation tank with a relatively low inlet concentration by considering several classes of particles, each characterized by a constant settling velocity. Although their transport model simulates the effects of densiometric forces on the flow field, the discrete settling model cannot account for hindered settling conditions of highly concentrated suspensions. Despite such numerous numerical studies, few papers considered the interaction between the biological reactor and the sedimentation units.

This work presents a model which takes into account the complete system. The proposed model can then be easily used as a tool for the design and management of activated sludge systems in wastewater treatment plants. The velocity field and the suspended solid concentration in the vertical plan of symmetry of the circular secondary sedimentation basins are solved by means of the differential equations describing the turbulent flow and the suspended solids transport in cylindrical coordinates. Modification of solid concentration values at the inlet of the sedimentation tank are considered by means of a mass balance model on both the substrate and biomass in the oxidation tank [30]. The numerical study is supported by measuring the sludge characteristics and the velocity field in a real circular sedimentation tank at an existing wastewater treatment plant in Rome. Attention has been given to the system resulting from the combination of the aerated reactor and the secondary clarifier to determine the influence of any variation in the biological sludge characteristics on the removal efficiency of the sedimentation unit by taking into account the actual velocity field established in the clarifier. Therefore, the numerical model calculates and modifies the flow field and the concentration

distribution in the sedimentation tank according to the sludge settling characteristics (i.e., varying the settling velocity or the boundary conditions) and the processes that take place inside of the activated sludge reactor. In this way, it is possible to consider the reactor–clarifier like an integrated system in which the operating efficiencies of the two units are mutually influenced and can also be used to define the best management actions. The efficiency of an activated sludge reactor depends on several aspects which have to be taken into account during the management phases to optimize the treatment results.

2. The "Biological Reactor–Clarifier" System as a Whole

In a biological wastewater treatment system, efficient performance of the secondary clarifier is essential because the system depends on the concentration of activated sludge available in the biological reactor. The purpose of the activated sludge recycled from the clarifier is then fundamental, as known, to maintain enough concentration of sludge in the reactor for reaching the required degree of treatment in an engineering valid time. Therefore, sludge recycled from the final clarifier to the inlet of the aeration tank is the essential feature of the process.

The performance of sedimentation units is strongly affected by several factors, such as the inlet concentration (X), the settling characteristics of the sludge, and last, but not least, the hydrodynamic field, which in turn depends on the sludge extraction, the geometrical characteristics of the basin, and the inflow. The scheme adopted in the model is reported in Figure 1.
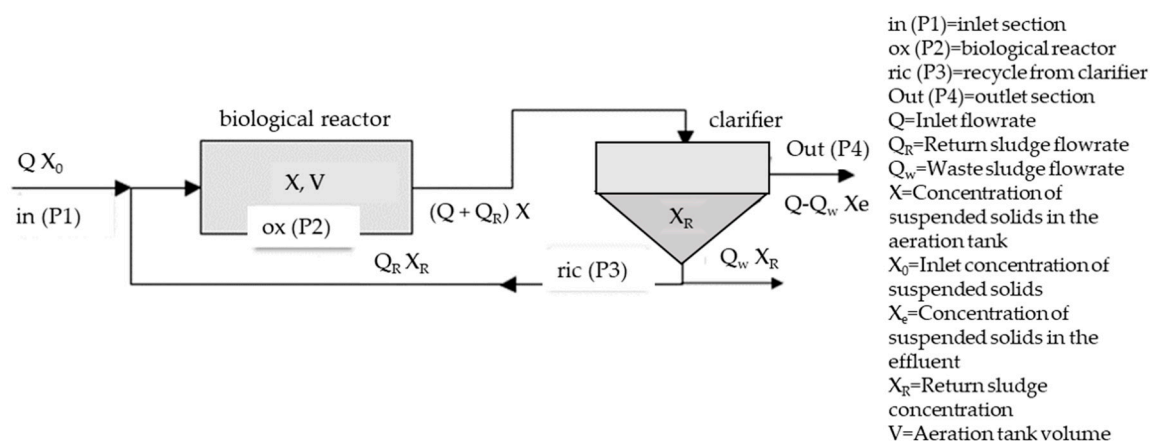

in (P1)=inlet section
ox (P2)=biological reactor
ric (P3)=recycle from clarifier
Out (P4)=outlet section
Q=Inlet flowrate
Q_R=Return sludge flowrate
Q_w=Waste sludge flowrate
X=Concentration of suspended solids in the aeration tank
X_0=Inlet concentration of suspended solids
X_e=Concentration of suspended solids in the effluent
X_R=Return sludge concentration
V=Aeration tank volume

Figure 1. Schematic of complete–mix reactor with cellular recycle and wasting from the recycle line.

A mass balance is used to evaluate both the biomass growth and the other management parameters.

Rate of accumulation of microorganism within the system boundary	=	Rate of flow of microorganism into the system boundary	−	Rate of flow of microorganism out of the system boundary	+	Net growth of microorganism within the system boundary

Mass balance for the microorganisms:

$$V\frac{dX}{dt} = QX_0 - [(Q - Q_w)X_e + Q_wX_R] + r'_gV. \tag{1}$$

Mass balance for the substrate:

$$V\frac{dS}{dt} = QS_0 - [(Q - Q_w)S + Q_wS] + r_{Su}V, \tag{2}$$

in which r'_g is the net growth of cells, S the substrate concentration, S_0 the substrate concentration in inlet wastewater, V the volume of the biological reactor, and r_{Su} the substrate utilization rate.

The following input data are required:

- Geometrical characteristics of the basins (biological reactor and clarifier);

Hydraulic loads: Inlet wastewater flowrate (Q), recirculated sludge flowrate (Q_R), and waste sludge flowrate (Q_W);

- Organic loads: Inlet chemical oxygen demand (COD) and biomass concentration in reactor.

The model allows simulating two different conditions:

Standard condition: The effective operating condition of the plant. It is possible to simulate the process efficiency (COD removal in the biological reactor, total suspend solids (TSS) concentration in the effluent from the clarifier) and the biomass concentration in the aerated reactor when hydraulic and organic loads are known.

Critical condition: The model allows to evaluate the optimal values of Q_R and Q_W to obtain a preset effluent substrate concentration. This option is useful when important variations of hydraulic and/or organic loads are expected to occur.

In Figure 2, a simplified scheme of the proposed model is shown. It is important to remark that it is possible:

- To modify the settling characteristics of the sludge by varying the coefficients in the settling velocity equation;
- To set input parameters (fitting of Q_R and Q_W) depending on the value of sludge concentration extracted from the clarified bottom (X_R).
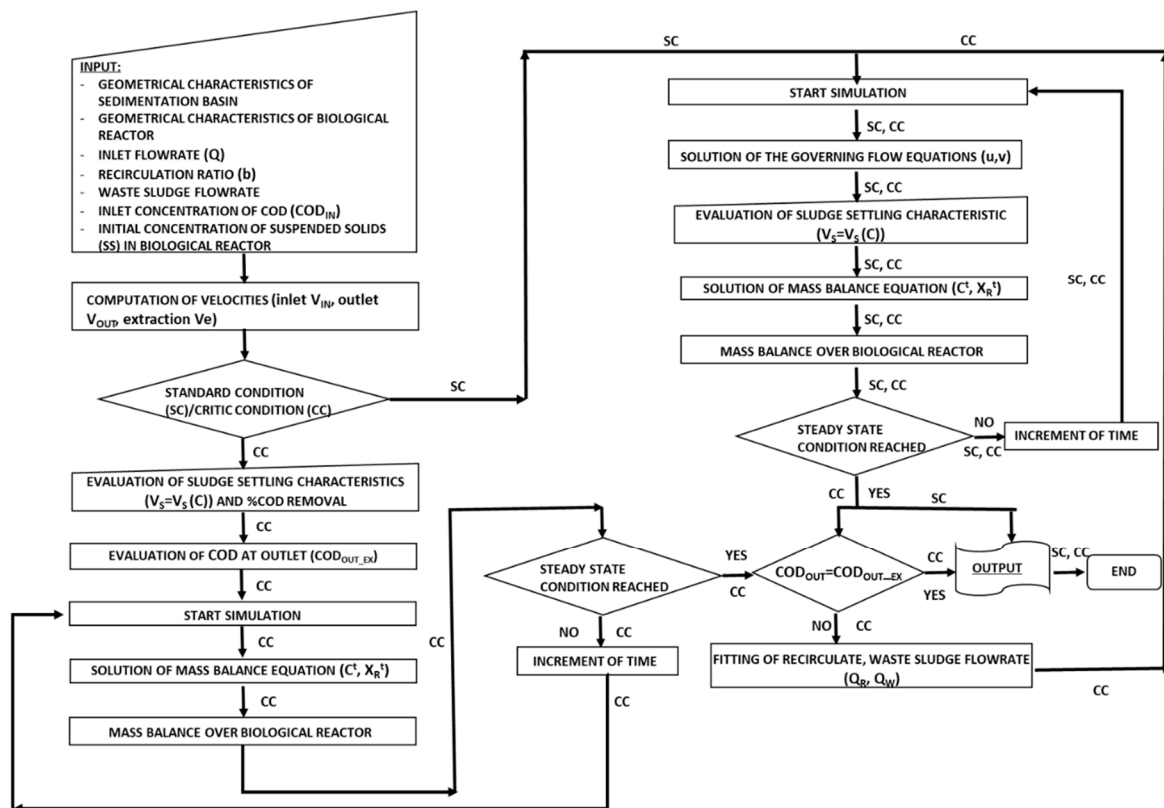

Figure 2. Flowchart of numerical model.

The presented model allows, therefore, evaluating the operating conditions in the biological reactor (the actual concentration of the biomass X and the waste amount) starting from defined

conditions in the sedimentation tank (X_R, Q_R). On the other hand, such conditions are dependent on the biomass concentration X at different times and on the waste sludge flowrate Q_w.

In this way, the biological reactor and the clarifier are mutually affected and behave like a single unit.

The velocity field and the sludge concentration distribution are simulated by means of the numerical integration of the Navier–Stokes equations in an axial symmetrical form. The sludge concentration distribution is solved by means of the mass balance equation to take into account the real phenomena of turbulence, transport, and diffusion. The model allows calculating:

- The velocity field in the sedimentation tank;
- The distribution of suspended solids (SS) concentration in the sedimentation tank;
- The SS concentration trend at the bottom of the clarifier;
- The SS concentration trend in the outlet section;
- The SS concentration trend in the biological reactor.

3. Simulation of Sedimentation Process

In the present study, the phenomena linked to thermal and concentration gradients were neglected and a not coupled procedure to reduce computational burden was adopted. In fact, the attention was principally focused on the management aspect (biological reactor–sedimentation tank system).

Several hypotheses are generally encountered in the literature [31] to allow for an easier numerical solution. One consists of the so called "rigid lid" approximation [10,23,24,28], which can be used thanks to the low values of the velocity.

3.1. Governing Equations

The equations describing axisymmetric, two-dimensional, unsteady, turbulent flow for cylindrical coordinates in a circular settling clarifier are:

The r-momentum equation:

$$\frac{\partial u}{\partial t} + u\frac{\partial u}{\partial r} + v\frac{\partial u}{\partial y} = -\frac{1}{\rho}\frac{\partial p}{\partial r} + \left(\frac{1}{r}\frac{\partial}{\partial r}\left(r\upsilon_t\frac{\partial u}{\partial r}\right) + \frac{1}{r}\frac{\partial}{\partial y}\left(r\upsilon_t\frac{\partial u}{\partial y}\right)\right), \tag{3}$$

the y-momentum equation:

$$\frac{\partial v}{\partial t} + u\frac{\partial v}{\partial r} + v\frac{\partial v}{\partial y} = -\frac{1}{\rho}\frac{\partial p}{\partial y} + \left(\frac{1}{r}\frac{\partial}{\partial r}\left(r\upsilon_t\frac{\partial v}{\partial r}\right) + \frac{1}{r}\frac{\partial}{\partial y}\left(r\upsilon_t\frac{\partial v}{\partial y}\right)\right), \tag{4}$$

and the continuity equation:

$$\frac{\partial ru}{\partial r} + \frac{\partial rv}{\partial y} = 0. \tag{5}$$

Symbols u and v represent mean velocity components in the r- and y-direction, respectively, p is the pressure, ρ the fluid density, and υt the eddy viscosity (which is considered constant and uniform inside the computational domain).

For a two-dimensional, unsteady flow, the convection–diffusion equation can be written as follows:

$$\frac{\partial C}{\partial t} + \frac{\partial (uC)}{\partial r} + \frac{\partial ((v - v_s)C)}{\partial y} = \left(\frac{1}{r}\frac{\partial}{\partial r}\left(rD_r\frac{\partial C}{\partial r}\right) + D_y\frac{\partial^2 C}{\partial y^2}\right), \tag{6}$$

where C is the suspended solids concentration, v_s is the settling velocity of suspended solids, D_r and D_y are the turbulent diffusion in the r-direction and y-direction, respectively. By using the Reynolds

analogy between mass transport and momentum transport, the dispersion coefficient is related to υ_t by:

$$D_r = \frac{\upsilon_t}{\sigma_{sr}}; \ D_y = \frac{\upsilon_t}{\sigma_{sy}}, \tag{7}$$

in which σ_{sr} and σ_{sy} are the Schmidt numbers (assumed equal 1.0) [28].

3.2. Computational Domain

The examined secondary clarifier is composed of a circular basin, with a central feeding system, having a total diameter of 52 m. The tank is equipped with a baffle located in proximity of the inlet section. The effluent outlet is realized through two weirs, one intermediate and one peripheral.

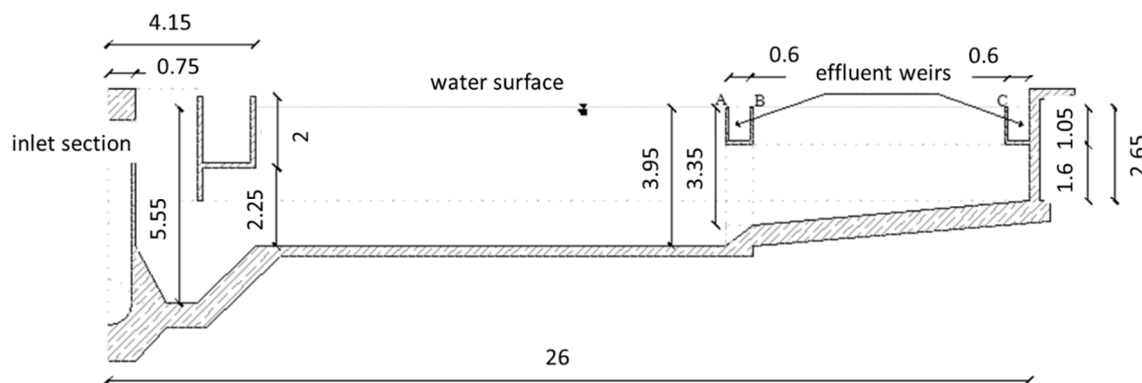The detailed characteristics of the basin are shown in Figure 3.

Figure 3. Vertical section of the circular clarifier.

After setting the system geometry within the integration domain, a square mesh grid was overlapped to it. The mesh dimensions are $\Delta r = \Delta y = 0.2$ m.

A dimensionless calculation domain was then obtained by dividing all the considered spatial variables by a reference length $l_0 = 4$m corresponding to the water head in the basin. Similarly, all other relevant variables (i.e., the coefficient of eddy viscosity υ_t and the velocities of the fluid (u,v) also referred to l_0, the inlet water velocity u_0, or $T_0 = l_0/u_0$ so as to obtain unit-less values.

3.3. Boundary Conditions

Solution of the partial equation set governing the phenomenon is only possible if a consistent series of boundary conditions are specified.

Inlet section. The profile is assigned starting from the fluid velocity at the inlet of the sedimentation basin. The assumed hypothesis is that such velocity has only the horizontal component u_{inlet}. The examined clarifier is in fact fed from the center with a capacity of approximately 1500 m^3/h. The recirculate flowrate has to be added to this value.

The profile of the suspended solids concentration is based on the relation:

$$(vC)_m = (vC)_v + \left(D_r \frac{\partial C}{\partial r} + D_y \frac{\partial C}{\partial y} \right)_v. \tag{8}$$

In this way, it is possible to transform a flow which is mainly convective into a convective–dispersive flow with energy losses and strong dispersion effects.

The inlet boundary condition for the concentration value is the Dirichlet condition. The assigned values are the fed substrate concentration and the reactor value of biomass concentration.

Free-surface boundary. The rigid lid approximation was used. The vertical component of velocity is then considered null.

As for the upper boundary condition, a null mass flux through the free surface of the water was imposed. This condition is mathematically represented as:

$$C(m, i) = 0. \tag{9}$$

Vertical walls. The model allows opened or closed contours. In the latter case, the adopted conditions are of impenetrability and "slip condition" for the flow and no mass flux for the solid's concentration.

Bottom of basin. It has been possible to define a series of boundary conditions able to ensure both fluid and solid mass conservation in the transport equation using considerations derived from mono-dimensional case studies. A single sedimentation column experiment allows fitting the correct boundary conditions. In the mono-dimensional case (vertical direction) the equation takes the form:

$$\frac{\partial C}{\partial t} + (v - v_s)\frac{\partial C}{\partial y} = D_y \frac{\partial^2 C}{\partial y^2}. \tag{10}$$

It is possible to neglect diffusion phenomena since no real hydrodynamic field is present; the transport equation then becomes:

$$\frac{\partial C}{\partial t} = v_s \frac{\partial C}{\partial y}, \tag{11}$$

introducing the flow $\phi = v_s C$:

$$\frac{\partial C}{\partial t} = \frac{\partial \phi}{\partial y}. \tag{12}$$

In this way the concentration variation with time is assumed to be dependent only on the flow differences along the vertical.

Such a model was applied to a sedimentation column test performed on a real sludge, and the results in terms of comparison between the position in time of the experimental interface height and the simulated one are shown in Figure 4.
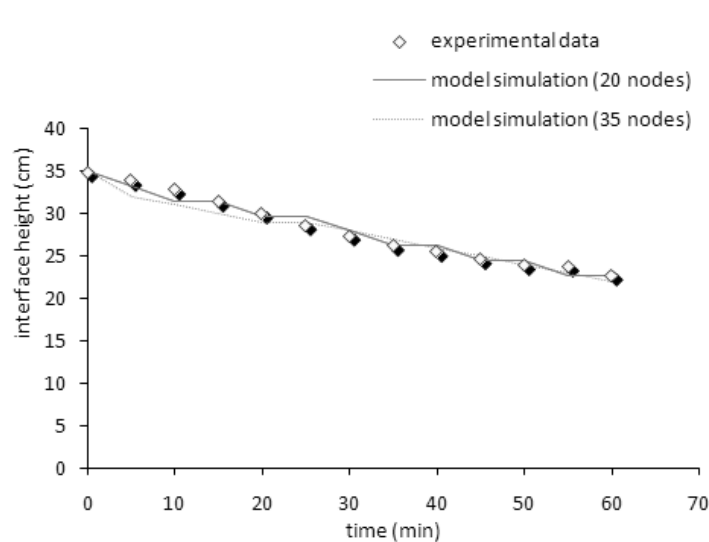

Figure 4. Interface height vs. time: Comparison between experimental data and model simulations.

The concentration at the bottom (in the node mm-1) is given by the relation:

$$C_{mm-1}^{t+1} = \frac{\Delta t}{\Delta y}\left(\phi_{mm-2}^t - \phi_{mm-1}^t\right) + C_{mm-1}^t. \tag{13}$$

A sludge flowrate is extracted from the bottom of the sedimentation tank to be recirculated or wasted. It is assumed, therefore, that the extracted flow is:

$$\phi^t_{mm-1} = v^t_e C^t_{mm-1},\tag{14}$$

where v_e is based on the extracted flowrate ($Q_R + Q_W$) and on the geometrical characteristics of the settler.

Outlet boundary.

It is considered as a weir with a hydraulic load equal to the vertical mesh dimension Δy.

3.4. Solution Procedure

In the present work, it was chosen to solve the equations governing the physical phenomenon in terms of primitive variables (u, v, p). Integration of the system of differential equations was realized through a semi-implicit finite differences algorithm (A.D.I. method).

4. Model Results

4.1. Comparison of Predicted and Experimental Velocities

The vectoral field of velocities in the basin (Figure 5) was calculated assuming that the speed of the water through the weirs is oriented only in the r direction.
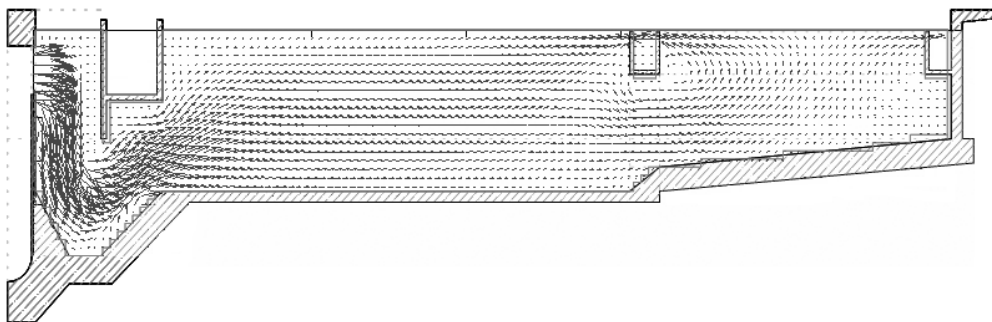

Figure 5. Velocity field: Comparison between experimental data and model simulations.

Several studies aimed at measuring the hydrodynamic field in sedimentation basins have shown that velocities values are between some millimeters and some centimeters per second [32,33]. In this study, such measures were carried out with an Argonaut ADV (Doppler 3D velocimeter) sensor in the circular secondary sedimentation tank at the wastewaters treatment plant of Roma Ostia (Italy).

The position of the measurement points was obviously decided based on the numerical discretization adopted, checking at every time that the main characteristics (inlet, Q_w, Q_R) could be considered rather constant; this allowed reaching a time-averaged flow field, which was used to calibrate the numerical model.

A representative test case is shown in Figure 6, where measurements and numerical simulations of the horizontal velocity profiles are compared. The agreement between experiments and numerical model is quite good, although the values calculated by the model in the central zone of the basin are quite higher than those observed at the field. This might be due to the presence of settled sludge, which can modify the actual section.

4.2. Settling Velocity of Suspended Solids

The settling of discrete, non-flocculating particles can be analyzed by means of the classic Stokes' sedimentation law. Particles in a relatively diluted solution will not act as discrete particles but will rather coalesce during sedimentation. As flocculation occurs, the mass of particles increases, and they

settle faster. As the ambient sediment concentration increases, the interparticle spacing is reduced, so the chance of particle collisions increases. This means that the settling velocity of the suspension will decrease when the concentration increases.
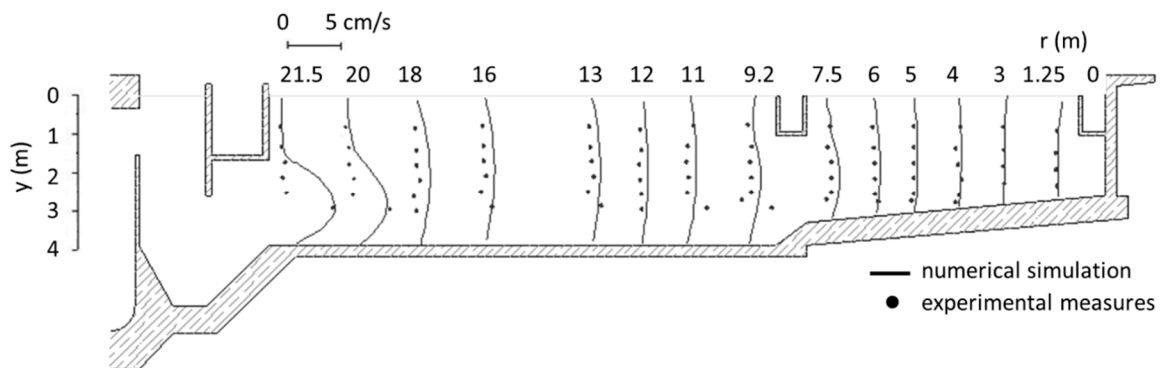

Figure 6. Profile of horizontal velocity: Comparison between experimental measures and numerical simulation.

A reasonable description of the complete settling process should be a settling rate that initially increases to a maximum, then decreases with increasing of concentration.

A large number of empirical formulas were proposed to describe the relationship between solids concentration and solids settling velocity; such relations generally assume the form of an exponential curve which fits particularly well the second part of the curve:

$$v_s = v_0 e^{-kC}, \tag{15}$$

where v_0 is the Stokes velocity and k is an empirical coefficient.

A series of batch-settling tests were conducted, and the results (summarized in Figure 7) show that the exponential formula can be successfully fitted to experimental data obtained at concentrations higher than 2000 mg/l.
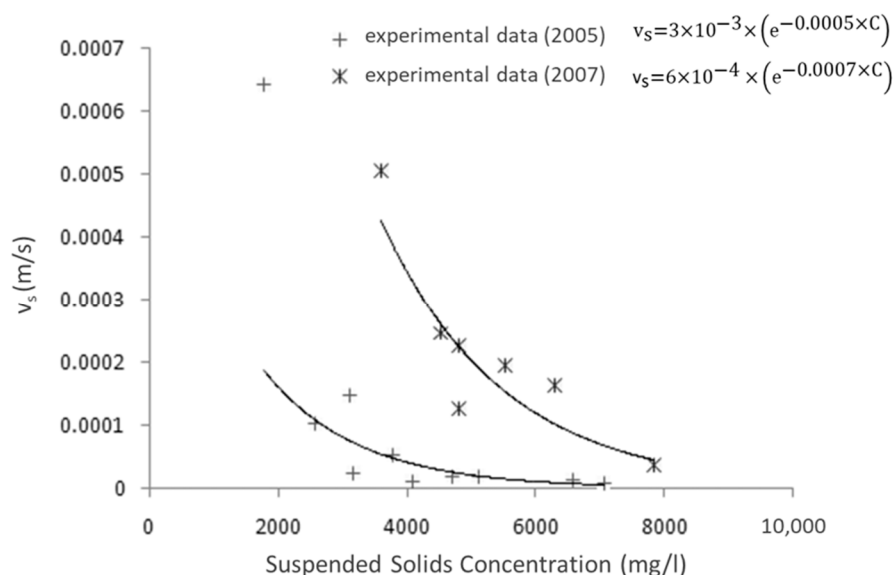

Figure 7. Experimental data of settling velocity.

The presented numerical model enables to vary the settling characteristics of the sludge and, therefore, the constants present in the relation used to describe the velocity. In such way, it is possible to estimate the effects of the sludge characteristics on the concentration field in the clarifier.

The calculation procedure is allowed to start with an empty (from solids) tank; sludge is entirely recirculated in the oxidation tank until a prefixed value of X is reached.

The mean residence time inside the basin is approximately 4 h; therefore, the adopted simulation time is about 5 h. It was in fact observed that the variation of the concentration's distribution does not turn out to be meaningful when carrying out extended simulations (because the steady state conditions are reached).

In the present work, two simulations were carried out by varying the sedimentation velocity of solid particles:

case (a)　$v_s = 3 \times 10^{-3} \times \left(e^{-0.0005 \times C}\right)$ (m/s) to simulate good settling characteristics of the sludge (experimental data 2007);

case (b)　$v_s = 6 \times 10^{-4} \times \left(e^{-0.0007 \times C}\right)$ (m/s) to simulate worse settling characteristics of the sludge (experimental data 2005).

In Figure 8a,b, the concentration distribution fields of suspended solid calculated with the above values for the settling velocity are reported. Both simulations were carried out in the same conditions of sludge extraction from the bottom (recirculation ratio b = 1) and with equal coefficients of diffusivity ($\Delta r = \Delta y = 0.001$). The basin fills up when the settling characteristics of the sludge get worse. The iso-concentration curves raise from the bottom and approach the outlet section.
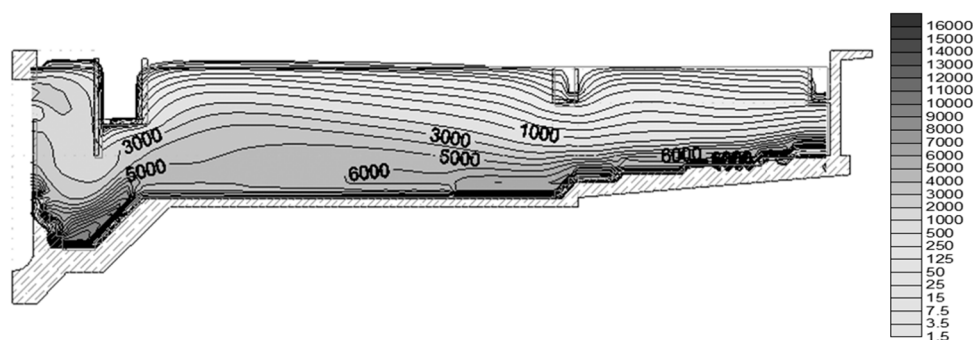
(**a**) $v_s = 3 \times 10^{-3} \times \left(e^{-0.0005 \times C}\right)$ (m/s)
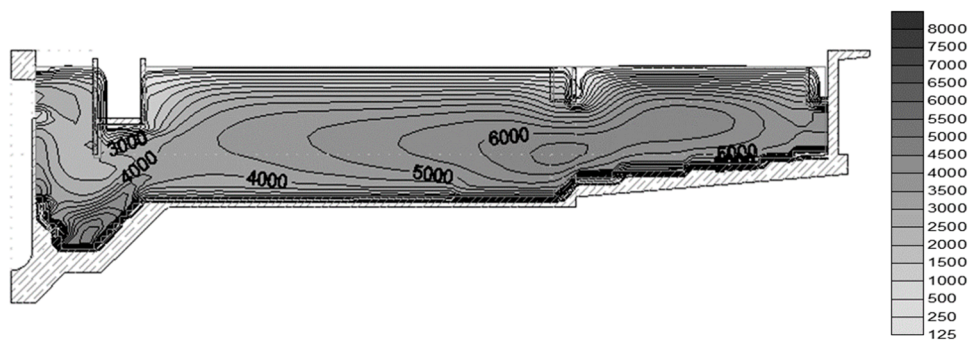
(**b**) $v_s = 6 \times 10^{-4} \times \left(e^{-0.0007 \times C}\right)$ (m/s)

Figure 8. Iso-concentration lines.

Noticeably, a non-negligible increase in the concentration values at the outlet nodes is observed (Figure 9a,b), until a steady state condition is reached after approximately 2 h of simulation. In particular, the difference of one order of magnitude in the sedimentation velocity v_0 determines twice a change in the values of concentration in the outlet nodes.

(**a**) $v_s = 3 \times 10^{-3} \times \left(e^{-0.0005 \times C} \right)$ (m/s)

(**b**) $v_s = 6 \times 10^{-4} \times \left(e^{-0.0007 \times C} \right)$ (m/s)
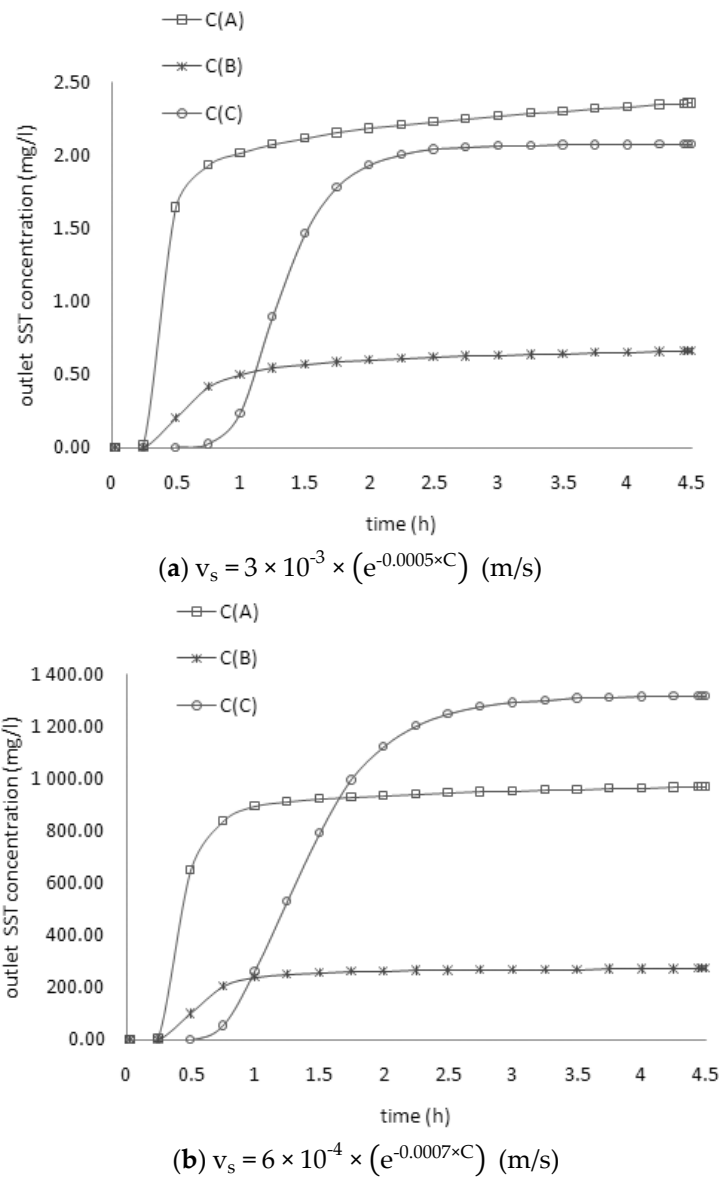
Figure 9. Concentration trend at the outlet nodes.

A balance between the mass present in the basin after 4 hours of simulation and the one of the basin inlets was provided to verify the reliability of the obtained results. Results shown in Table 1 are based on the concentrations reported in Table 2.

Table 1. Mass balance in the sedimentation tank.

	$v_0 = 3 \times 10^{-3}$ m/s	$v_0 = 6 \times 10^{-4}$ m/s
	Mass (kg)	**Mass (kg)**
inlet	36,000	36,000
inside tank	22,694	33,427
outlet	0.0662	39.97
extract	16,104.49	2711.26
TOTAL	**38798**	**36178**

Table 2. Calculated suspended solids (SS) concentration in the clarifier.

	$v_s=3\times10^{-3}\times(e^{-0.0005\times C})$ (m/s)	$v_s=6\times10^{-4}\times(e^{-0.0007\times C})$ (m/s)
	Concentration (mg/l)	Concentration (mg/l)
inside tank	2922.26	4304.39
bottom	7097.58	74,089.05
surface	23.51	1103.43

The model allows for any variation of Q_R and Q_W to be considered depending on the sludge concentration (X) in the biological reactor. According to the variation of such flowrates, the flow field and the distribution of suspended solids concentration are calculated with respect to the new conditions of inlet, outlet, and extraction.

4.3. Biological Reactor–Clarifier System

In a first stage, a series of numerical simulation were carried out for a deep evaluation of model sensitivity to the operative parameters and for defining the most significative period to be adopted for the experimental data collection.

Figure 10a,b shows the biomass growth inside the reactor until a prefixed value is obtained ($X_{expected}$ = 3000 mg/l) and the related concentration at the sedimentation tank bottom (X_R) starting from an empty tank condition (X_R = 0) when a sludge with good sedimentation characteristics is considered. The removal of the exceeding biomass starts when the $X_{expected}$ is reached in the biological reactor. From Figure 10b, it is possible to observe the discontinuity point which marks the instant when sludge extraction begins.
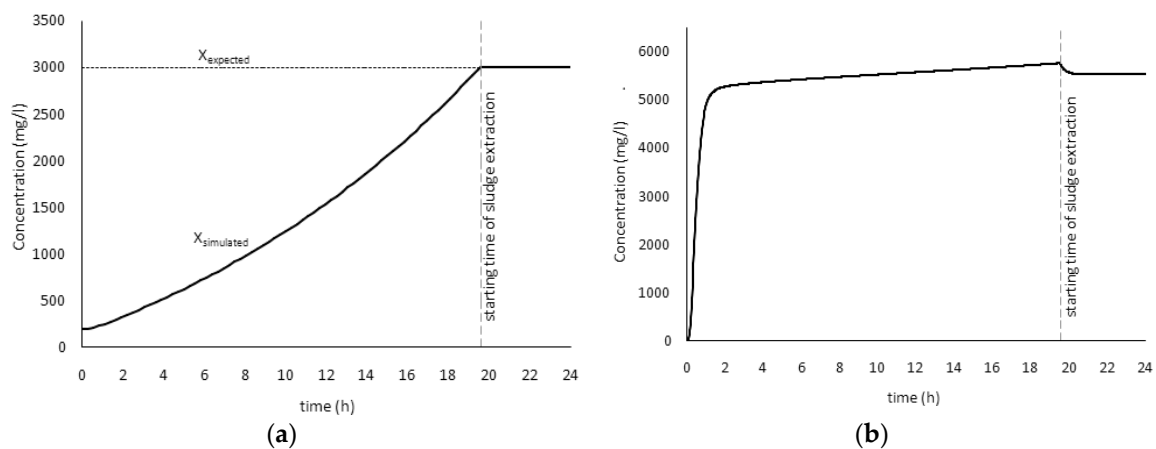

Figure 10. Mixed liquor suspended solids (MLSS) concentration trend in the biological reactor (**a**) and sludge concentration trend in the recirculate flowrate (**b**).

Following this, a series of tests were conducted to simulate the effects of a strong variation on the inlet COD concentration, which makes it necessary to operate an intervention on the sludge extraction flow or on the recycle flowrate. The model should allow modifying the values of the management parameters (sludge extraction and/or recycle of sludge) to reach correct operating conditions within the shortest feasible time.

The used initial conditions are:

- No solids in the clarifier;
- Initial COD concentration in the reactor equal to 50 mg/l;
- Initial mixed liquor volatile suspended solids (MLVSS) concentration in the reactor equal to 2890 mg/l;

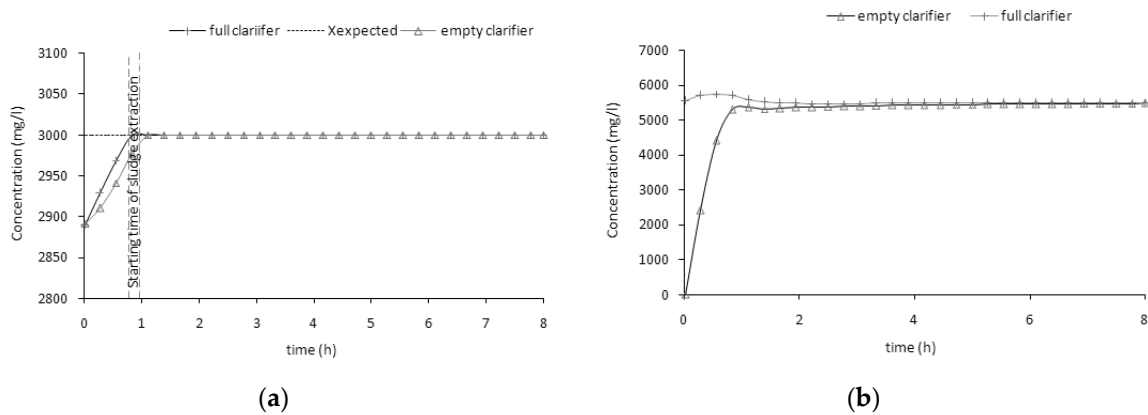Figure 11a,b shows the biomass concentration in the reactor vs. time for two different operative conditions.

(a)   (b)

Figure 11. Mixed liquor suspended solids (MLSS) concentration trend in the biological reactor (**a**) and sludge concentration trend in the recirculate flowrate (**b**).

By observing the profiles, it is possible to analyze the reliance of the biomass growth linked to the kinetic parameter in the reactor but also to the recycling concentration [34]. Such a low value of X_R can bring a strong dilution effect in the biomass concentration in the biological reactor, especially if this lasts for a long time (i.e., the time which is needed to define the interventions).

Figure 12a,b shows the COD vs. time in the reactor and the sludge extraction flowrate, which changes depending on the inlet organic load and, consequently, the biomass growth.
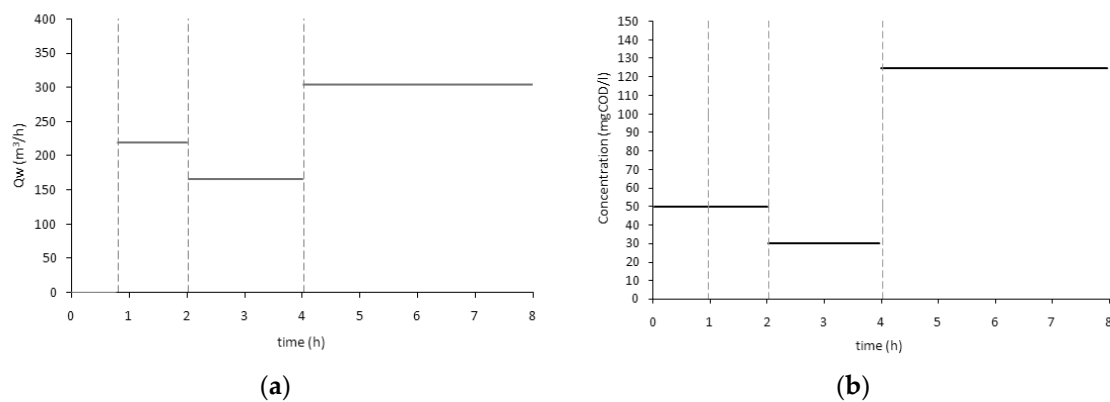

(a)   (b)

Figure 12. Waste sludge flowrate (**a**) and substrate concentration trend in the biological reactor (**b**).

Sludge extraction rate adjustment represents an operative intervention frequently used in the treatment plant management; it is necessary when high variation in the organic load occurs.

The calibration and validation of the model was based on three different phases: The first two were devoted to the evaluation of the characteristic parameters (calibration phase), the last one to validate the numerical model. The calibration of the flow field parameter was pointed on the turbulent diffusion coefficient (regarding the velocity field, the flow at the outlet could guarantee, in this phase, the calibration results), and velocities measured on the real sedimentation tank were used. To allow for direct comparison with model results, field measures were taken instantaneously at defined sampling locations. For the transport model, the sedimentation characteristics of the sludge were derived from the column tests, and for the diffusion coefficients, very low values (due to the small turbulent effects present in the tank) were considered. In the end, a comparison with real data, derived from further direct measures on the sedimentation tank, was used for the validation phase.

Three experimental campaigns were carried out. Analysis of the chemical values and of flow at the inlet, recycling flow, and sludge extraction flow were measured at the sampling points shown in Figure 1.

　P1 = inlet section

　P2 = biological reactor

　P3 = recycle from clarifier

　P4 = outlet section

A numerical simulation was carried out for each campaign, and the results are shown in the following paragraphs.

Campaign 1. The first campaign was aimed at defining the kinetic constants for the organic substance removal.

COD at the inlet and at the outlet, TSS in the oxidation tank, in the recycle flow, and at the outlet were measured and a volatile suspended solids (VSS)/TSS rate equal to 0.75 was calculated.

In Table 3, the hydraulic loads measured at the plant and used in the simulation are shown. The input value of COD is the average of the measured values.

Table 3. Experimental values of hydraulic loads.

	Unit	Campaign 1	Campaign 2	Campaign 3
Q	m^3/h	2631	2662	2956
Q_R	m^3/h	3178	3180	2692
Q_w	m^3/d	1680	1680	1680
θ_h	h	3.20	3.82	3.39
b		1.21	1.19	from 1.20 to 0.9

The obtained data were used as input parameters to the numerical model and for the calibration phase. The following values were assigned to the kinetic constants:

- Y = 0.45 mgVSS/mgCOD;
- K_d = 0.08 d^{-1};
- k_s = 80 mgCOD/l;
- K = 2.0 d^{-1};

The assigned values were evaluated by means of several runs until a minimum value of the quadratic mean error could be reached.

In the following graphs, the comparison between experimental data and calculated values of COD (Figure 13a) and TSS (Figure 13b,c) concentration in the different sections of the system is reported.
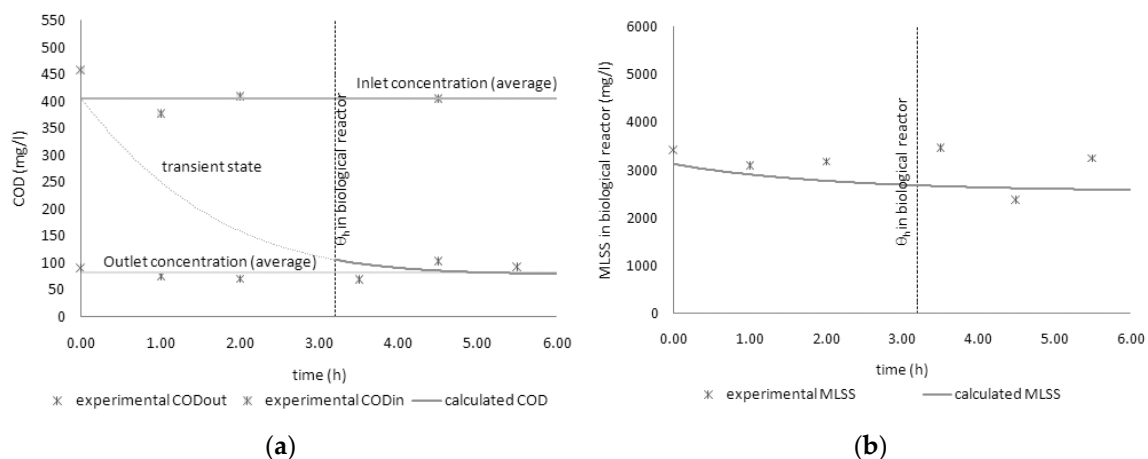

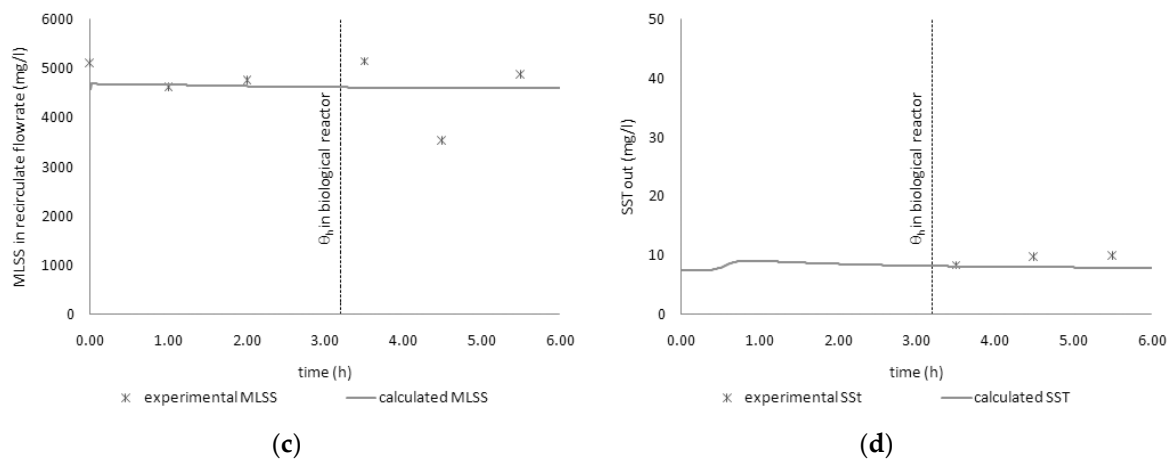(a)　　　　　　　　　　　　　　　　　　　　　　　(b)

Figure 13. *Cont.*

(**c**)

(**d**)

Figure 13. Campaign 1: Chemical oxygen demand (COD) concentration (**a**) and total suspend solids (TSS) concentration in biological reactor (**b**), in recycling flowrate (**c**), and in the effluent (**d**).

Campaign 2. The values of the kinetic parameters obtained in the first campaign were then also used in this second test. In the following graphs, the numerical simulation results vs. the experimental values for COD (Figure 14a) and TSS (Figure 14b–d) are shown.
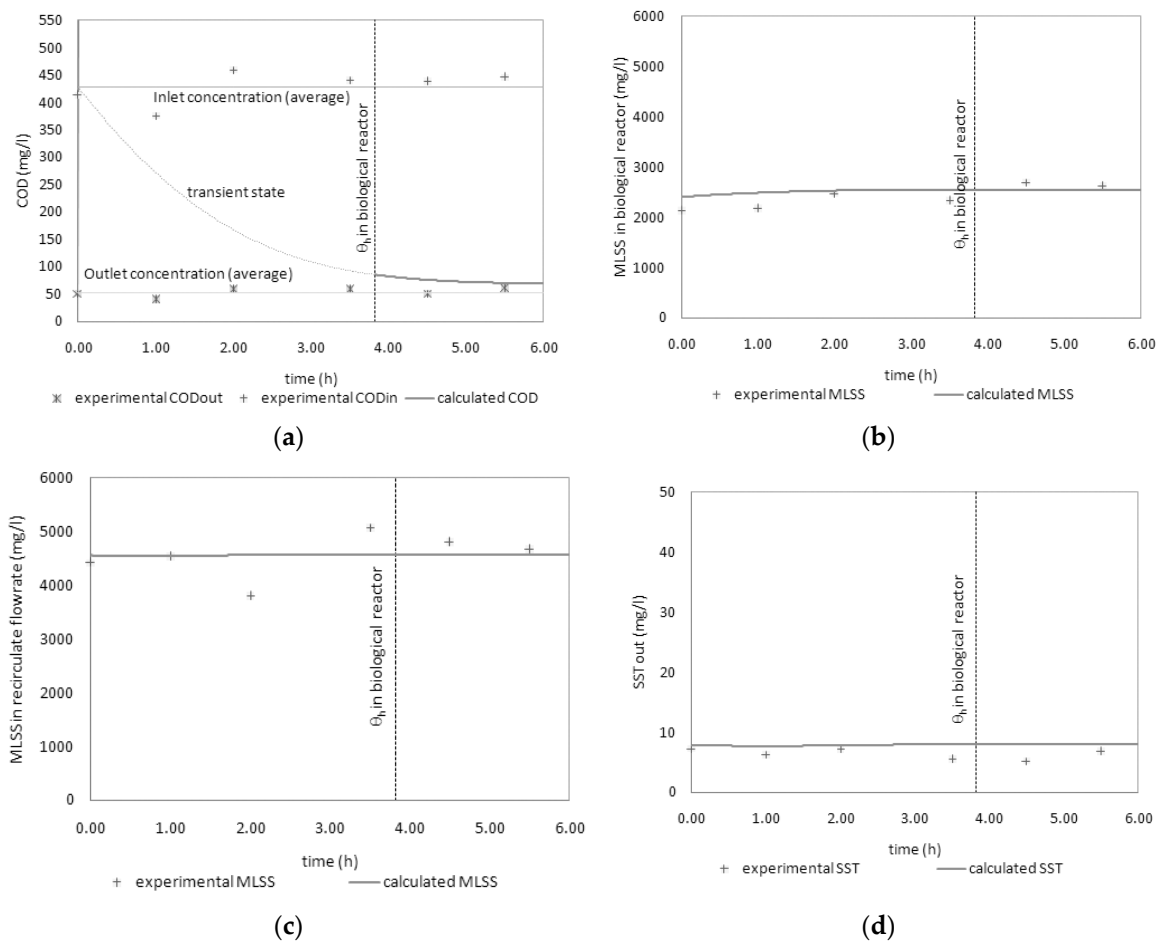

(**a**)

(**b**)

(**c**)

(**d**)

Figure 14. Campaign 2: COD concentration (**a**) and TSS concentration in biological reactor (**b**), in recycling flowrate (**c**), and in the effluent (**d**).

Campaign 3. In this case, a reduction of the recycle flowrate value (b = 1.2 until 0.9, Table 3) was imposed to the plant management. As shown from the analysis of the reported profiles (Figure 15a–d),

the numerical model forecasts a reduction of the TSS concentration in the reactor and, consequently, an increase of the COD concentration at the outlet. The comparison between the experimental values (sampling obtained on the day after) shows the same trend predicted by the numerical model.
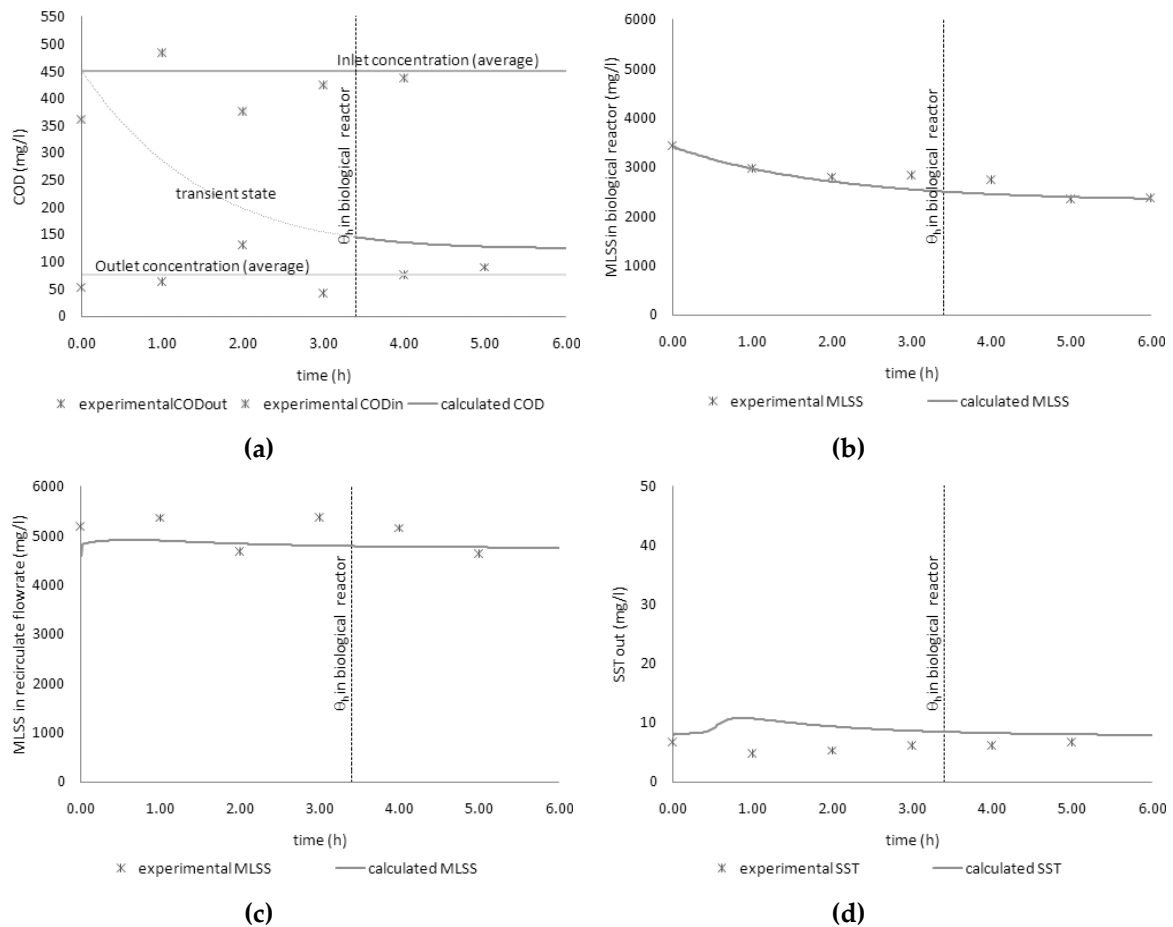

(a)

(b)

(c)

(d)

Figure 15. Campaign 3: COD concentration (**a**) and TSS concentration in biological reactor (**b**), in recycling flowrate (**c**), and in the effluent (**d**)).

The compared error analysis for the three considered cases, shown in Table 4, indicates that simulated values fit experimental ones well, except for the case of COD, where the model provides overestimated values, particularly in the second and third campaigns.

Table 4. Quadratic mean error.

	Campaign 1	Campaign 2	Campaign 3
COD in P4	6.42%	19.80%	32.76%
TSS in P2	6.06%	2.51%	2.60%
TSS in P3	4.81%	8.93%	3.18%
TSS in P4	9.17%	3.50%	21.97%

5. Conclusions

The paper is not intended to introduce new concepts about wastewater treatment but rather aimed at overcoming the classical methods used to design and manage wastewater treatment plants, with respect to the activated sludge system. Once the geometrical characteristics of the biological reactor and of the clarifier have been fixed, monitoring inlet COD concentrations is enough to control

eventual problems which can occur in the case of sudden variations of the organic or hydraulic loads. By measuring the sludge main characteristics, the best sludge extraction or the best recycle flow may be evaluated, allowing for significant energy saving, especially for big plants.

Management strategies suitable to face any variation in the inlet or in the sludge settling characteristics can be defined in a short time by selecting the most effective intervention based on the results provided by the proposed numerical model. The calibration and validation phases have shown the validity of this approach, which considers the reactor–clarifier system as a whole. The response time of the numerical model was confirmed by the analysis carried out on a real plant, and the eventual correction to be operated in to reach the standard efficiency values for the plant could be evaluated in a few hours without attempting to correct the trend based solely on empirical experience.

Author Contributions: Conceptualization, F.T. and S.C.; methodology, P.V., F.T., and S.C.; software, F.T. and S.C.; validation, P.V., V.T., F.T., and S.C.; formal analysis, F.T.; investigation, S.C.; resources, P.V.; data curation, S.C.; writing—original draft preparation, S.C.; writing—review and editing, S.C. and N.F.; visualization, S.C.; supervision, V.T. and P.V.; project administration, P.V.

Nomenclature

$b = Q_R/Q$	Recirculation ratio [-]
C	Concentration [$M \cdot L^{-3}$]
COD	Chemical oxygen demand [$M \cdot L^{-3}$]
D_r	Coefficient of diffusivity (r direction) [$L^2 \cdot T^{-1}$]
D_y	Coefficient of diffusivity (y direction) [$L^2 \cdot T^{-1}$]
e	Nepero number [-]
k	Empirical coefficient [-]
l_0	Water head in the basin [L]
MLVSS	Mixed liquor volatile suspended solids [$M \cdot L^{-3}$]
MLSS	Mixed liquor suspended solids [$M \cdot L^{-3}$]
p	Pressure [$M \cdot T^{-2} \cdot L^{-1}$]
Q	Inlet flowrate [$L^3 \cdot T^{-1}$]
$Q_e = Q - Q_w$	Outlet flowrate (from biological reactor) [$L^3 \cdot T^{-1}$]
Q_R	Return sludge flowrate [$L^3 \cdot T^{-1}$]
Q_w	Waste sludge flowrate [$L^3 \cdot T^{-1}$]
r	Horizontal coordinate [L]
r'_g	Net growth of cells [T^{-1}]
r_{su}	Substrate utilization rate [T^{-1}]
S	Substrate concentration [$M \cdot L^{-3}$]
S_0	Substrate concentration in inlet wastewater [$M \cdot L^{-3}$]
SS	Suspended solids [$M \cdot L^{-3}$]
TSS	Total suspend solids [$M \cdot L^{-3}$]
$T_0 = l_0/u_0$	Time interval [T]
u	Mean velocity component (r direction) [$L \cdot T^{-1}$]
u_0	Water inlet velocity [$L \cdot T^{-1}$]
v	Mean velocity component (y direction) [$L \cdot T^{-1}$]
v_e	Sludge extraction velocity [$L \cdot T^{-1}$]
v_0	Stokes velocity [$L \cdot T^{-1}$]
v_s	Settling velocity [$L \cdot T^{-1}$]
V	Aeration tank volume [L^3]
y	Vertical coordinate [L]
X	Concentration of suspended solids in the aeration tank [$M \cdot L^{-3}$]
X_e	Concentration of suspended solids in the effluent [$M \cdot L^{-3}$]

X_0	Inlet concentration of suspended solids [M· L^{-3}]
X_R	Return sludge concentration [M· L^{-3}]
$\Delta r, \Delta y$	Mesh dimensions [L]
$\phi = vC$	Flow (y direction) [M·T^{-1}· L^{-2}]
υ_t	Eddy viscosity coefficient [L^2·T^{-1}]
ρ	Fluid density [M·L^{-3}]
σ_{sr}	Schmidt numbers (r direction) [-]
σ_{sy}	Schmidt numbers (y direction) [-]

References

1. Takamatsu, T.; Naito, M.; Shiba, S.; Ueda, Y. Effects of deposit resuspension on settling basin. *J. Environ. Eng. Div.* **1974**, *100*, 883–903.
2. Larsen, P. *On the Hydraulic of Rectangular Settling Basins: Experimental and Theoretical Studies*; Report n. 1001; Department of Water Resources Engineering, Lund Institute of Technology: Lund, Sweden, 1977.
3. Abdel-Gawad, S.; McCorquodale, J. Numerical simulation of rectangular settling tanks. *J. Hydraul. Res.* **1985**, *23*, 85–100. [CrossRef]
4. Wang, X.; Yang, L.; Sun, Y.; Song, L.; Zhang, M.; Cao, Y. Three-dimensional simulation on the water flow field and suspended solids concentration in the rectangular sedimentation tank. *J. Environ. Eng.* **2008**, *134*, 902–911. [CrossRef]
5. Al-Sammarraee, M.; Chan, A.; Salim, S.M.; Mahabaleswar, U.S. Large-eddy simulations of particle sedimentation in a longitudinal sedimentation basin of a water treatment plant. Part I: Particle settling performance. *J. Chem. Eng.* **2009**, *152*, 315–321. [CrossRef]
6. Gong, M.; Xanthos, S.; Ramalingam, K.; Fillos, J.; Beckmann, K.; Deur, A.; McCorquodale, J.A. Development of a flocculation sub-model for a 3-D CFD model based on rectangular settling tanks. *Water Sci. Technol.* **2011**, *63*, 213–219. [CrossRef]
7. Schamber, D.R.; Larock, B.E. Numerical analysis of flow in sedimentation basins. *Hydr. Div. ASCE* **1981**, *107*, 575–591.
8. Rodi, W. Turbulence models and their application in Hydraulics. A state–of–the–art review. *NASA STI/Recon Tech. Rep. A* **1980**, *81*, 1–115.
9. Stamou, A.I.; Adams, E.W.; Rodi, W. Numerical modelling of flow and settling in primary rectangular clarifiers. *J. Hydraul. Res.* **1989**, *27*, 665–682. [CrossRef]
10. Armbruster, M.; Krebs, P.; Rodi, W. Numerical modelling of dynamic sludge blanket behaviour in secondary clarifiers. *Water Sci. Technol.* **2001**, *43*, 173–180. [CrossRef] [PubMed]
11. Kleine, D.; Reddy, B.D. Finite element analysis of flows in secondary settling tanks. *Int. J. Numer. Method. Biomed. Eng.* **2005**, *64*, 849–876. [CrossRef]
12. Weiss, M.; Plósz, B.G.; Essemiani, K.; Meinhold, J. Suction-lift sludge removal and non-Newtonian flow behaviour in circular secondary clarifiers: Numerical modelling and measurements. *J. Chem. Eng.* **2007**, *132*, 241–255. [CrossRef]
13. Tamayol, A.; Firoozabadi, B.; Ashjari, M. Hydrodynamics of secondary settling tanks and increasing their performance using baffles. *J. Environ. Eng.* **2009**, *136*, 32–39. [CrossRef]
14. Patziger, M.; Kainz, H.; Hunze, M.; Jozsa, J. Influence of secondary settling tank performance on suspended solids mass balance in activated sludge systems. *Water Res.* **2012**, *46*, 2415–2424. [CrossRef]
15. Xanthos, S.; Ramalingam, K.; Lipke, S.; McKenna, B.; Fillos, J. Implementation of CFD modeling in the performance assessment and optimization of secondary clarifiers: The PVSC case study. *Water Sci. Technol.* **2013**, *68*, 1901–1913. [CrossRef]
16. Ramin, E.; Wagner, D.S.; Yde, L.; Binning, P.J.; Rasmussen, M.R.; Mikkelsen, P.S.; Plosz, B.G. A new settling velocity model to describe secondary sedimentation. *Water Res.* **2014**, *66*, 447–458. [CrossRef]
17. Gao, H.; Stenstrom, M.K. Evaluation of three turbulence models in predicting the steady state hydrodynamics of a secondary sedimentation tank. *Water Res.* **2018**, *143*, 445–456. [CrossRef]
18. Imam, E.; McCorquodale, J.A.; Bewtra, J.K. Numerical modelling of sedimentation tanks. *J. Hydraul. Eng.* **1983**, *109*, 1740–1754. [CrossRef]

19. Adams, E.; Rodi, W. Modeling flow and mixing in sedimentation tanks. *J. Hydraul. Eng.* **1990**, *116*, 895–913. [CrossRef]

20. Mazzolani, G.; Pirozzi, F. Modello numerico di sedimentazione per sospensioni con densità uniforme. *Ingegneria Sanitaria* **1995**, *43*, 15–33.

21. Goula, A.M.; Kostoglou, M.; Karapantsios, T.D.; Zouboulis, A.I. A CFD methodology for the design of sedimentation tanks in potable water treatment case study: The influence of a feed flow control baffle. *J. Chem. Eng.* **2008**, *140*, 110–121. [CrossRef]

22. DeVantier, B.A.; Larock, B.E. Modelling sediment-induced density currents in sedimentation basins. *J. Hydraul. Eng.* **1987**, *113*, 80–94. [CrossRef]

23. Zhou, S.; McCorquodale, J.A.; Vitasovic, Z. Influence of skirt radius on performance of circular clarifier with density stratification. *Int. J. Numer. Methods Fluids* **1992**, *14*, 919–934. [CrossRef]

24. Zhou, S.; McCorquodale, J.A.; Vitasovic, Z. Influences of density on circular clarifiers with baffles. *J. Environ. Eng.* **1992**, *118*, 829–847. [CrossRef]

25. Al-Sammarraee, M.; Chan, A. Large-eddy simulations of particle sedimentation in a longitudinal sedimentation basin of a water treatment plant. Part 2: The effects of baffles. *J. Chem. Eng.* **2009**, *152*, 315–321. [CrossRef]

26. Byonghi, L. Evaluation of Double Perforated Baffles Installed in Rectangular Secondary Clarifiers. *Water* **2017**, *9*, 407. [CrossRef]

27. Mazzolani, G.; Pirozzi, F.; D'Antonio, G. A generalized settling approach in the numerical modelling of sedimentation tanks. *Water Sci. Technol.* **1998**, *38*, 95–102. [CrossRef]

28. Zhou, S.; McCorquodale, J.A. Modelling of rectangular settling tanks. *J. Hydraul. Eng.* **1992**, *118*, 1391–1405. [CrossRef]

29. Lyn, D.A.; Stamou, A.I.; Rodi, W. Density currents and shear-induced flocculation in sedimentation tanks. *J. Hydraul. Eng.* **1992**, *118*, 849–867. [CrossRef]

30. Luciano, A.; Viotti, P.; Mancini, G.; Torretta, V. An integrated wastewater treatment system using a BAS reactor with biomass attached to tubolar supports. *J. Environ. Manag.* **2012**, *113*, 51–60. [CrossRef]

31. Szalai, L.; Krebs, P.; Rodi, W. Simulation of flow in circular clarifiers with and without swirl. *J. Hydraul. Eng.* **1994**, *120*, 4–21. [CrossRef]

32. Bertola, P. Campo di velocità e distribuzione della concentrazione del fango nella vasca di sedimentazione finale di un impianto di depurazione. *Ingegneria Sanitaria* **1980**, *6*, 318–332.

33. Bretscher, U.; Krebs, P.; Hager, W.H. Improvement of flow in final settling tanks. *J. Environ. Eng.* **1992**, *118*, 307–321. [CrossRef]

34. Torretta, V.; Ragazzi, M.; Trulli, E.; De Feo, G.; Urbini, G.; Raboni, M.; Rada, E.C. Assessment of biological kinetics in a conventional municipal WWTP by means of the oxygen uptake rate method. *Sustainability* **2014**, *6*, 1833–1847. [CrossRef]